Title Page

Altered PKC Regulation of Pulmonary Endothelial Store- and Receptor-Operated Ca^{2+} Entry Following Chronic Hypoxia

Michael L. Paffett, Melissa A. Riddle, Nancy L. Kanagy, Thomas C. Resta and Benjimen R. Walker

Vascular Physiology Group

Department of Cell Biology and Physiology (M.L.P., M.A.R., N.L.K., T.C.R., B.R.W.)

University of New Mexico Health Sciences Center Albuquerque, NM 87131-0001

JPET Fast Forward. Published on June 24, 2010 as DOI: 10.1124/jpet.110.165563
This article has not been copyedited and formatted. The final version may differ from this version.

Running Title Page

a) Running Title: Endothelial Ca^{2+} Entry Following Chronic Hypoxia

b) Address Correspondence to: Michael L. Paffett, PhD.
Dept. of Cell Biology and Physiology
1 University of New Mexico
MSC08 4750
Albuquerque, NM 87131
Phone: (505) 272-0622
Fax: (505) 272-6649
Email: Mpaffett@salud.unm.edu

c) Number of Text Pages: 17
Number of Tables: 0
Number of Figures: 8
Number of References: 36
Number of Words
Abstract: 235
Introduction: 659
Discussion: 1841

d) Chronic hypoxia (CH), endothelial cell (EC), store-operated Ca^{2+} (SOC), cyclopiazonic acid (CPA), 1-oleoyl-2-acetyl-*sn*-glycerol (OAG), receptor-operated Ca^{2+} (ROC), sarco/endoplasmic reticulum Ca^{2+} ATPase (SERCA), voltage-gated Ca^{2+} channel (VGCC), vascular smooth muscle (VSM), transient receptor potential (TRP), diacylglycerol (DAG),

e) Section Assignment: Cardiovascular

JPET Fast Forward. Published on June 24, 2010 as DOI: 10.1124/jpet.110.165563
This article has not been copyedited and formatted. The final version may differ from this version.

Abstract

Chronic hypoxia (CH)-induced pulmonary hypertension is associated with decreased basal pulmonary artery endothelial cell (EC) Ca^{2+} which correlates with reduced store-operated Ca^{2+} (SOC) entry. PKC attenuates SOC entry in ECs. Therefore, we hypothesized that PKC has a greater inhibitory effect on EC SOC and receptor-operated Ca^{2+} entry following CH. To test this hypothesis, we assessed SOC in the presence or absence of the non-selective PKC inhibitor GF109203X in freshly isolated, fura-2 loaded ECs obtained from intrapulmonary arteries of control and CH rats (4 wk at 0.5 atm). We found that SOC entry as well as OAG- and ATP-induced Ca^{2+} influx were attenuated in ECs from CH rats vs. controls and GF109203X restored SOC and OAG responses to the level of controls. In contrast, non-selective PKC inhibition with GF109203X or the selective PKC_{ε} inhibitor, V1-2myr, attenuated ATP-induced Ca^{2+} entry in ECs from control, but not CH pulmonary arteries. ATP-induced Ca^{2+} entry was also attenuated by the T-type voltage-gated Ca^{2+} channel (VGCC) inhibitor, mibefradil, in control cells. Consistent with the presence of endothelial T-type VGCC, we observed depolarization-induced Ca^{2+} influx in control cells that was inhibited by mibefradil. This response was largely absent in ECs from CH arteries. We conclude that CH enhances PKC-dependent inhibition of SOC and OAG-induced Ca^{2+} entry. Furthermore, these data suggest that CH may reduce the ATP-dependent Ca^{2+} entry that is mediated, in part, by PKCε and mibefradil-sensitive Ca^{2+} channels in control cells.

Conditions associated with chronic hypoxia (CH), such as chronic bronchitis and emphysema, often lead to pulmonary hypertension. The endothelium is an important regulator of pulmonary vascular tone that may be affected by CH. It has been recently observed that basal endothelial cell (EC) $[Ca^{2+}]_i$ and store-operated Ca^{2+} (SOC) entry are reduced in pressurized intrapulmonary arteries from CH rats (Paffett et al., 2007). Since many vasodilatory pathways, such as the production of nitric oxide and prostacyclin, are Ca^{2+}-dependent, diminution of $[Ca^{2+}]_i$ could promote the vasoconstriction observed in this setting. However, the mechanism of reduced EC Ca^{2+} entry following CH has not been investigated. The present study examines the role of PKC in reduced Ca^{2+} entry.

Many families of ion channels in a variety of cell types are regulated by PKC. Some of the first reports of PKC modulating voltage-gated Ca^{2+} channels (VGCCs) were in neuronal (Ewald et al., 1988;Yang and Tsien, 1993) and vascular smooth muscle (VSM) preparations (Schuhmann and Groschner, 1994). These early investigations revealed that stimulating PKC with phorbol esters can either potentiate or inhibit VGCC activity depending on the cell type or concentration of PKC agonist. More recently, thrombin-induced activation of T-type VGCCs has been characterized in the pulmonary microvasculature (Wu et al., 2003) and shown to be involve PKC_ε (Park et al., 2006). In addition to modulating VGCC, PKC can also target transient receptor potential (TRP) channels in the vasculature. For example, Earley et al. (2007) observed PKC-dependent activation of the mechanosensitive TRPM4 isoform that contributes to control of cerebral vascular tone. PKC also regulates members of the canonical sub-family of TRP channels known to be expressed in vascular endothelium and smooth muscle. TRPC1/4/5 isoforms are activated by depletion of intracellular Ca^{2+} stores resulting in extracellular

JPET Fast Forward. Published on June 24, 2010 as DOI: 10.1124/jpet.110.165563
This article has not been copyedited and formatted. The final version may differ from this version.

Ca^{2+} influx or SOC entry, whereas TRPC3/6/7 are believed to be activated in a store-independent manner by a variety of second-messenger systems and are often referred to as receptor-operated Ca^{2+} (ROC) entry [see review; Pedersen, S.F. et al. 2005 (Pedersen and Nilius, 2007)]. PKC has been identified as both an activator of SOC entry in portal vein (Albert and Large, 2002) and an inhibitor in pulmonary artery VSM cells (Horibe et al., 2001), but there is little information regarding the role of PKC in modulating SOC and ROC entry in the vascular endothelium.

PKC isoforms are classified into three categories determined by their NH_2-terminal regulatory domain structure. Conventional PKCs (cPKCs; α, β_I, β_{II} and γ) contain a C1 domain that binds diacylglycerol (DAG) and a C2 domain that binds anionic phospholipids in a Ca^{2+}-dependent manner. Novel PKCs (nPKCs; δ, θ, ε and η) are activated by DAG, but not by changes in cytosolic Ca^{2+}. Unlike conventional and novel PKCs, atypical PKCs (aPKCs; ζ and ι/λ) are characterized as DAG and Ca^{2+}-insensitive, but activated by phosphatidylinositol trisphosphate or ceramide [see review; (Gallegos and Newton, 2008)]. Whereas most PKC sub-families and their respective isoforms are ubiquitously expressed throughout various tissues, their regulatory actions on SOC and ROC entry vary widely. For example, PKC_α contributes to activation of SOC entry in cultured mesangial (Ma et al., 2002) and ECs (Ahmmed et al., 2004). Similarly, δ and β PKC isoforms are required for SOC entry in corneal epithelium (Zhang et al., 2006). More recently, Yang et al. (Yang et al., 2008) found that non-specific inhibition of PKC enhanced SOC entry in pulmonary artery VSM, suggesting an inhibitory rather than a potentiating role within the pulmonary vasculature. These reports highlight the diverse

JPET Fast Forward. Published on June 24, 2010 as DOI: 10.1124/jpet.110.165563
This article has not been copyedited and formatted. The final version may differ from this version.

effects of PKC on SOC entry in the non-pathological setting, however little is known about the role of PKC regulation of EC SOC and ROC entry following CH.

Therefore, we hypothesized that reduced EC SOC and ROC entry following CH are mediated by altered PKC-dependent regulation. We tested this hypothesis by examining the effect of different PKC inhibitors on SOC and ROC entry in freshly isolated endothelium from intrapulmonary arteries from control rats and pulmonary hypertensive animals exposed to 4 weeks of CH.

Methods

All protocols used in this study were reviewed and approved by the Institutional Animal Care and Use Committee of the University of New Mexico Health Sciences Center.

Exposure of Rats to Chronic Hypoxia.

Male Sprague-Dawley rats (Harlan Industries; 200-250g) were used for all studies. CH exposure consisted of housing rats in a pressure controlled environment (~380 torr) for 4 weeks. Age-matched control rats were boarded in similar cages under ambient barometric pressure (~630 torr). The hypobaric chamber was opened 3 times/wk to provide fresh rat chow, water and clean bedding.

Isolation and Preparation of Pulmonary Artery Endothelial Cells

Rats were euthanized with sodium pentobarbital (200 mg kg^{-1} i.p.) and the left lung rapidly excised and placed in HEPES buffered saline solution (HBSS). The HBSS

contained the following (in mM): 150 NaCl, 6 KCl, 1 $MgCl_2$, 1.8 $CaCl_2$, 10 HEPES, and 10 glucose, titrated to pH 7.4 with NaOH. Intrapulmonary arteries (3^{rd} and 4^{th} order, 200-400 μm internal diameter) were dissected from the cranial most region of the left lung and carefully cleaned of surrounding lung parenchyma. Endothelial sheets were enzymatically dissociated and stored for up to 5 hours at 4°C as previously described (Paffett et al., 2007). Freshly isolated rat pulmonary artery endothelial cells were then placed on a poly-L-lysine coated glass bottom 35 mm culture dish (BD Biosciences) with a small bore fire-polished Pasteur pipette and allowed to equilibrate for 30 min at room temperature prior to experimentation.

Fura-2 Loading of Freshly Isolated Endothelial Sheets

Ca^{2+} entry was determined in freshly isolated endothelial sheets using the ratio-metric Ca^{2+} sensitive dye fura-2 AM (Invitrogen). Endothelial sheets were loaded with fura-2 AM (3 μM and 0.05% pluronic acid) in HBSS for 5 min at ~23°C and washed for 15 min at 37°C. Ratiometric changes in endothelial cell $[Ca^{2+}]_i$ were acquired by alternating specimen excitation for 50 msec between 340 and 380 nm bandpass filters at 1 Hz (Ionoptix Hyperswitch) in which the interleaved fura-2 emissions at 510 nm were detected with a photomultiplier tube.

JPET Fast Forward. Published on June 24, 2010 as DOI: 10.1124/jpet.110.165563
This article has not been copyedited and formatted. The final version may differ from this version.

Assessing the Role of PKC-Dependent Modulation of SOC and ROC Entry

Following a 30 min recovery period and fura-2 loading, endothelial sheets were superfused with HBSS at 37°C and then switched to Ca^{2+}-free HBSS (equimolar Mg^{2+} substitution) for 2-3 min. Passive depletion of intracellular Ca^{2+} stores by inhibition of the sarco/endoplasmic reticulum Ca^{2+} ATPase (SERCA) with cyclopiazonic acid (CPA, 10 μM) was performed and SOC entry was defined as the change in 340/380 fluorescence after repletion of extracellular Ca^{2+} (Figure 1). After the SOC entry response, stabilized ROC entry was assessed by the addition of (OAG, 100 μM) or ATP (20 μM) in the continued presence of CPA. Any further increase in fura-2 ratio was defined as ROC entry (Figure 1) as previously described (Jernigan et al., 2006). In separate experiments, ROC entry was assessed in cells pre-incubated for 10 min with the non-specific inhibitor of PKC (GF109203X, 1 μM) prior to the re-application of extracellular Ca^{2+} and ROC entry agonist. In parallel experiments, the cell permeant PKC_{ε} peptide inhibitor (myrV1-2, 10 μM) or a concentration specific $PKC_{\alpha/\beta}$ inhibitor (Gö6976, 6 nM) was applied for period of 10 min prior to the addition of ATP.

Effect of Ca^{2+} Channel Blockers on ATP-induced Ca^{2+} Entry

To determine if ATP-induced ROC entry is mediated by voltage-dependent Ca^{2+} channels, we examined Ca^{2+} responses to ATP in store-depleted endothelial cells from control and CH arteries pre-incubated with the putative T-type Ca^{2+} channel inhibitor mibefradil (10 μM); the L-type Ca^{2+} channel inhibitor diltiazem (50 μM); the non-selective Ca^{2+} channel blocker SKF96365 (20 μM) or vehicle for 5 min prior stimulation with ATP. These concentrations of diltiazem and mibefradil have been previously

JPET Fast Forward. Published on June 24, 2010 as DOI: 10.1124/jpet.110.165563
This article has not been copyedited and formatted. The final version may differ from this version.

reported to selectively inhibit L- and T-type VGCCs, respectively (Zhou et al., 2007;Wei et al., 2004). Furthermore, we performed validation experiments using patch clamp techniques to confirm the selective inhibitory actions of mibefradil and diltiazem in neonatal cardiomyocytes and pulmonary artery vascular smooth muscle cells, respectively (see Supplemental Figures 1 and 2).

Role of PLC, Mibefradil-Sensitive Ca^{2+} Channels and PKC_ε in ATP-Induced Ca^{2+} Entry

Additional experiments were conducted to confirm that ATP-induced Ca^{2+} entry involves PLC initiated signaling events. Following the development of a stable SOC entry response, 20 μM ATP was added in the presence of the PLC inhibitor U73122 (3 μM) or its inactive analog U73343 (3 μM). To corroborate the involvement of T-type Ca^{2+} channels in ATP-induced entry, parallel experiments were performed in the presence of mibefradil. Furthermore, to determine if PKC_ε and T-type Ca^{2+}channel activation were operating in parallel following the addition of ATP, we assessed ATP-induced Ca^{2+} influx in the presence of mibefradil and the myristoylated V1-2 peptide PKC_ε inhibitor.

Endothelial Ca^{2+} Responses to Extracellular KCl

Since results of the above studies suggested the presence of endothelial VGCCs, the response to depolarizing concentrations of KCl (15, 30, 60 and 90 mM) was assessed in cells from control and CH rats. Parallel experiments were performed in which 5 μM of the KCl selective ionophore valinomycin was present to rule out the possibility of unequal K^+ conductance differentially regulating E_m between groups. To determine the

JPET Fast Forward. Published on June 24, 2010 as DOI: 10.1124/jpet.110.165563
This article has not been copyedited and formatted. The final version may differ from this version.

potential involvement of L- and T-type voltage sensitive Ca^{2+} channels, a 60 mM KCl depolarizing stimulus was applied in the presence or absence of the respective inhibitors, diltiazem and mibefradil. Furthermore, to rule out any potential tonic influences of store-operated Ca^{2+} entry on the depolarizing effects of KCl, these experiments were conducted in the presence of CPA to inhibit SERCA.

Qualitative Immunofluorescence of $Ca_v3.1$ (α1G) in the Pulmonary Endothelium

Freshly isolated pulmonary arterial endothelium from control or CH animals were fixed in 4% paraformaldehyde at room temperature for 10 min. After fixation, all samples were permeabilized with 0.01% Triton X-100 PBS for 10 min and blocked with 3% donkey serum in PBS for 1 hour at room temperature. Fixed cells were incubated with primary antibodies for the $Ca_v3.1$ (α1G) T-type VGCC subunit (1:100, rabbit polyclonal) and PECAM-1 (1:200, mouse monoclonal) (Transduction Laboratories) overnight at 4°C. Respective primary antibodies were detected with Cy5-conjugated donkey anti-rabbit and Cy3-conjugated donkey anti-mouse secondary antibodies (1:500 dilution – Jackson Laboratories).Nuclei were stained with Sytox (1:10,000 dilution – Molecular Probes) and applied to all samples. Specimens were visualized with a confocal laser microscope (LSM 510 Zeiss) with a 63x oil immersion lens.

Calculations and Statistics

All data are expressed as means ± S.E. Values of *n* refer to the number of endothelial sheets (40-100 cells/sheet) in which 1-2 sheets were studied from one rat. A one-way or two-ANOVA was used where appropriate for all comparisons between

JPET Fast Forward. Published on June 24, 2010 as DOI: 10.1124/jpet.110.165563
This article has not been copyedited and formatted. The final version may differ from this version.

control and CH groups. If differences were detected by ANOVA, individual groups were compared with the Student-Newman-Keuls test. A probability of ≤ 0.05 was accepted as statistically significant for all comparisons.

Results

Differential PKC Regulation of SOC- and ROC entry

Both SOC and ROC entry were diminished in cells from CH compared to control arteries (Figure 2). Diminished ROC entry was seen both in experiments employing OAG (Figure 2) and those utilizing ATP (Figure 3) as an agonist. Non-selective PKC inhibition with GF109203X restored both SOC and OAG-induced Ca^{2+} entry in endothelial cells isolated from CH arteries to the level of controls without affecting the control group (Figures 2A and B). In contrast, GF109203X reduced ATP-induced Ca^{2+} responses in endothelial cells from control arteries (Figure 3). Similarly, PKC_{ε} inhibition with V1-2myr effectively blunted ATP-induced Ca^{2+} entry in control endothelium, whereas $PKC_{\alpha/\beta}$ inhibition with Gö6976 had no effect. In contrast to control cells, neither pan-specific inhibition of PKCs, nor selective $PKC_{\alpha/\beta}$ or PKC_{ε} inhibition affected the blunted ATP-induced Ca^{2+} response in the CH group. These results demonstrate that CH exposure results in a generalized reduction in Ca^{2+} entry, however there appears to be differential regulation by various PKC isoforms depending upon the mode of activation.

Effect of Ca^{2+} Channel Blockers on ATP-induced Ca^{2+} Entry

Inhibition of T-type Ca^{2+} channels with mibefradil blunted ATP-induced Ca^{2+} entry in endothelial cells from control rats compared to vehicle but was without effect in

JPET Fast Forward. Published on June 24, 2010 as DOI: 10.1124/jpet.110.165563
This article has not been copyedited and formatted. The final version may differ from this version.

cells from CH rats (Figure 4). Similarly, the non-selective inhibitor of voltage-dependent Ca^{2+} channels SKF96365 reduced entry only in control cells. In contrast, L-type Ca^{2+} channel inhibition was ineffective at blocking ROC entry in either group.

Role of PLC, Mibefradil-Sensitive Ca^{2+} Channels and PKC_{ε} in ATP-Induced Ca^{2+} Entry

Experiments were performed with U73122 to verify that ATP-induced responses involved PLC-initiated events. PLC inhibition with U73122 abolished ATP-induced Ca^{2+} responses in endothelial cells from both control and CH arteries whereas the inactive analog U73343 of this inhibitor had no effect (Figure 5). Furthermore, as seen in previous protocols, mibefradil reduced ROC entry in the control group only. When mibefradil was combined with the PKC_{ε} inhibitor, V1-2myr, no additive effect was observed. Interestingly, neither of these inhibitors had an effect on ATP-induced Ca^{2+} entry in endothelial cells from CH arteries.

Endothelial Ca^{2+} Responses to Extracellular KCl

Application of increasing concentrations of extracellular KCl increased endothelial cell Ca^{2+} in control cells (Figure 6A), however this response was greatly attenuated in ECs from CH arteries (Figure 6B). These differences persisted when endothelial K^+ permeability and hence E_m was equivalently clamped with valinomycin across all KCl concentrations (Figure 6C), demonstrating that unequal K^+ permeability does not account for the observed differences between groups. Additional experiments showed that the Ca^{2+} response to 60 mM KCl was inhibited by the T-type antagonist mibefradil in control cells, but had no effect in cells from CH rats. The L-type channel

JPET Fast Forward. Published on June 24, 2010 as DOI: 10.1124/jpet.110.165563
This article has not been copyedited and formatted. The final version may differ from this version.

inhibitor diltiazem did not affect either group. These data suggest that a mibefradil-sensitive (T-type VGCCs) account for depolarization-induced Ca^{2+} entry in control cells and that this response is lost following CH.

Qualitative Immunofluorescence of $Ca_v3.1$ (α1G) in the Pulmonary Endothelium

$Ca_v3.1$ immunofluorescence was detected in the endothelium from control rats and appeared to be peripherally located (Figure 7-*top panel*). Immunofluorescence was also detected in endothelium from CH vessels; however $Ca_v3.1$ fluorescence appeared to be less abundant at the cell periphery (Figure 7-*middle panel*). Primary antibody specificity was confirmed with the blocking antigen and endothelial cells were positively identified by a PECAM-1 label (Figure 7-*bottom panel*).

Discussion

The present study illustrates the differential regulation of endothelial SOC and ROC entry pathways by PKC following CH-induced pulmonary hypertension. The major findings of this study are: *1)* SOC entry, OAG- and ATP-induced Ca^{2+} influx pathways are attenuated in freshly dissociated endothelium from CH pulmonary arteries compared to controls; *2)* non-selective inhibition of PKC restores SOC and OAG responses in endothelium from CH rats to the level of controls; *3)* PKC_ε inhibition attenuates ATP-induced Ca^{2+} entry in endothelium from control, but not CH pulmonary arteries; 4) ATP-induced Ca^{2+} entry was inhibited by mibefradil in control but not CH endothelia; and 5) CH attenuates high K^+-induced Ca^{2+} entry whereas this response was present control ECs and blocked by mibefradil. Taken together, these findings suggest that CH

upregulates PKC-dependent inhibition of SOC and OAG-induced Ca^{2+} entry. Furthermore, these data also suggest that CH reduces PLC-dependent Ca^{2+} entry that appears to be mediated, in part, by PKC_{ε} and mibefradil sensitive Ca^{2+} channels in control cells. Impaired Ca^{2+} entry following CH could significantly diminish production and release of important vasodilatory mediators thereby exacerbating the severity of pulmonary hypertension.

In most cells, receptor-dependent activation of PLC stimulates the production of IP_3 and subsequent release of Ca^{2+} from intracellular stores which leads to plasmalemmal Ca^{2+} influx. The store-dependent arm of this signaling pathway is activated by IP_3 binding to IP_3 receptors, depleting ER Ca^{2+} and stimulating SOC entry. However, there is considerable evidence that PLC-dependent DAG production mediates store-independent Ca^{2+} influx (Cheng et al., 2006;Leung et al., 2006). The present study demonstrates that endothelial cells from small pulmonary arteries possess store-independent Ca^{2+} entry elicited by either OAG or ATP application following CPA-induced store depletion (Figure 2B). Furthermore, our results are consistent with studies that suggest DAG directly activates TRPC channels in endothelial cells (Pocock et al., 2004). In addition to exogenous DAG analogues, endogenous DAG has been shown to stimulate Ca^{2+} influx independent of PKC activation (Trebak et al., 2003;Gamberucci et al., 2002). The current understanding from these reports and others is that DAG stimulates TRPC3/6/7 isoforms leading to Ca^{2+} influx but that TRPC1/4/5 isoforms are not involved, [reviewed in (Pedersen and Nilius, 2007)] in DAG-dependent Ca^{2+} influx. Interestingly, our results show reduced OAG- and ATP-dependent Ca^{2+} entry is reduced in CH-induced pulmonary hypertension.

JPET Fast Forward. Published on June 24, 2010 as DOI: 10.1124/jpet.110.165563
This article has not been copyedited and formatted. The final version may differ from this version.

The role of DAG-activated PKC in regulating SOC/ROC entry is controversial. Broad-spectrum PKC activators inhibit SOC entry in human neutrophils (Montero et al., 1993) and SOC entry-mediated photoreceptor activation (Hardie et al., 1993) in *Drosophila*. Furthermore, Venkatachalam et al. (2003) demonstrated that $PLC_{\gamma 2}$-dependent activation of TRPC3/4/5 Ca^{2+} influx is negatively regulated by PKC secondary to cytosolic Ca^{2+} and/or DAG accumulation following receptor activation. Similarly, our findings suggest that PKC inhibits SOC- and OAG-induced Ca^{2+} entry following CH (Figure 2A and B), however this mechanism was not evident in endothelial cells from control rats.

To further characterize the effects of CH on ROC entry and how PKC may be regulating Ca^{2+} influx, we examined purinergic receptor stimulated Ca^{2+} influx. Consistent with effects on SOC entry and OAG-induced Ca^{2+} influx, we found ATP-induced Ca^{2+} influx was decreased in CH compared to control endothelia. Although we observed a similar decrease in Ca^{2+} influx to SOC- and OAG-induced Ca^{2+} entry following CH, it appears that purinergic receptor activation may lead to a distinct signaling cascade requiring PKC activation to stimulate ROC entry in control endothelial cells only (Figure 3). Similar findings by Lee et al. (1997) found that 30 μM ATP promoted PKC-dependent activation of ROC entry, whereas 300 μM ATP evoked PKC-dependent inhibition of this response. This earlier report suggests PKC activates Ca^{2+} influx at concentrations of ATP similar to those employed in the current study. The apparently opposing roles for PKC in regulating endothelial cell ROC entry depending upon the mode of activation (*i.e.* OAG vs. ATP) suggests that different signaling cascades are activated by these approaches. Pharmacological characterization of ATP-

induced Ca^{2+} entry revealed that PKC_{ε} appears to be a key regulator in control cells but that this mode of activation may be lost following CH. Although this possibility is likely, the use of sub-maximal concentrations of Ca^{2+} channel and/or PKC inhibitors could influence our conclusion that CH impairs Ca^{2+} influx. However, the concentrations of mibefradil and diltiazem utilized were effective at abolishing Ca^{2+} currents in cells known to express the targeted channels (see Supplemental Figures 1 and 2). Thus, the residual Ca^{2+} influx mediated by KCl- and ATP may represent diltiazem- and mibefradil-insensitive Ca^{2+} entry pathways that are still intact in endothelial cells from either experimental group. This interpretation of residual Ca^{2+} entry is further supported by the finding that PLC blockade abrogates ATP-induced Ca^{2+} influx in control as well as CH endothelial cells (Figure 5) suggesting either PKC inhibitor concentrations were sub-maximal (particularly $PKC_{\alpha/\beta}$ inhibition with Gö6976) or intact Ca^{2+} entry pathways not regulated by PKCs accounting for this residual Ca^{2+} influx.

CH could decrease PLC activity or PKC_{ε} activity, thereby limiting downstream activation of ROC entry. Information concerning altered PLC and PKC_{ε} activities in the pulmonary endothelium following CH is limited. However, attenuated PLC-dependent Ca^{2+} mobilization in myometrial smooth muscle exposed to hypobaric hypoxia has been reported (Arakawa et al., 2004). Additionally, acute hypoxic exposure decreases phosphoinositide synthesis in carotid bodies (Rigual et al., 1999). More recent studies demonstrate increased PKC_{α} and PKC_{δ} expression, but reductions in $PKC_{\beta II}$, PKC_{γ}, and PKC_{ε} in hypertrophied right ventricles from CH rats (Uenoyama et al., 2010), suggesting differential effects on PKC expression by CH. Although this recent finding supports the differential regulation of various PKC isoforms by CH, further investigation into the

effects of CH on pulmonary endothelial PKC and the disparate roles they play in regulating Ca^{2+} influx is warranted.

Until recently, there has been limited support for the existence and/or role for T-type VGCCs in the pulmonary endothelium. However, molecular (De, I et al., 2007), biophysical and pharmacological (Wu et al., 2003) evidence of $Ca_v3.1$ T-type VGCCs in the pulmonary microcirculation supports our observation that endothelial cells freshly dissociated from small pulmonary arteries express functional T-type VGCCs. This conclusion was corroborated by demonstration of $Ca_v3.1$ T-type VGCC expression by immunofluorescence (Figure 7). However, our findings that KCl-induced Ca^{2+} entry is reduced (Figure 6B and C) and insensitive to the T-type channel inhibitor, mibefradil (Figure 6D) in endothelial cells from CH-hypertensive arteries indicate a functional and/or expressional sensitivity of this Ca^{2+} channel to CH.

A potential caveat of this interpretation is non-specific actions of mibefradil on L-type VGCCs. However, there was no effect of diltiazem on KCl-induced Ca^{2+} influx in endothelial cells from pulmonary normotensive rats (Figure 6) indicating a benzothiazepine(diltiazem)-insensitivity to depolarization-induced Ca^{2+} entry. Furthermore, the specific inhibitory actions of mibefradil and diltiazem were documented in neonatal cardiomyocytes and pulmonary artery vascular smooth muscle cells, respectively (see online data supplement). Similar patch clamp experiments were attempted in freshly dispersed endothelial sheets *(data not shown)*, but space-clamping prevented precise control of membrane potential as these cells appear to have intact intercellular communication leading to a very large capacitance proportional to the number of cells in a given sheet. Furthermore, we were unable to observe an inward

JPET Fast Forward. Published on June 24, 2010 as DOI: 10.1124/jpet.110.165563
This article has not been copyedited and formatted. The final version may differ from this version.

rectifying Ca^{2+} current with the classical biophysical (rapid activation and inactivation) signature of T-type VGCCs in electrically isolated single endothelial cells *(data not shown).* It is possible that the elusive nature of identifying T-type VGCCs in the single cell preparation is due to a small sub-population of endothelial cells that actually express T-type VGCCs. Unfortunately, these technical limitations prevented the complete dissection of the biophysical nature and pharmacology properties of the observed Ca^{2+} channels and the involved PKC isoforms.

In addition, our data suggest that depolarizing stimuli (high K^+) promote endothelial Ca^{2+} entry from control, but not from CH rats. This finding was somewhat surprising, since there is a lack of consensus that VGCCs exist in the pulmonary endothelium. Similar to the relatively absent KCl-induced Ca^{2+} influx following CH, we found that receptor-mediated (ATP) Ca^{2+} influx was also reduced following CH. These parallel observations of absent Ca^{2+} influx pathways led us to hypothesize that VGCCs are activated by purinoceptor stimulation. Therefore, it is possible that T-type VGCCs represent another mode of ROC entry that is sensitive to PKC activation. Consistent with this hypothesis are multiple findings (Chemin et al., 2007;Kim et al., 2007;Park et al., 2003;Park et al., 2006) illustrating that PKC activation stimulates $Ca_v3.1$ and $Ca_v3.2$ Ca^{2+} currents. Although the specific PKC isoforms modulating Ca^{2+} influx through T-type VGCCs were not determined in these prior reports, our data suggest that PKC_ε plays a role in stimulating Ca^{2+} influx in the pulmonary endothelium. Moreover, the lack of sensitivity to both V1-2myr, mibefradil and the inability of 60 mM KCl to elicit significant changes in Ca^{2+} influx in cells from CH rats compared to controls suggests that T-type VGCCs may be downregulated at the expressional level or possibly not

appropriately localized on the plasma membrane. Although this study did not examine ion channel trafficking or expression due to protein sample limitations, further experiments are needed to support these speculations.

It is also possible that ATP binds to P2X receptors leading to membrane depolarization through non-selective cation influx and activation of T-type Ca^{2+} channels. It is generally accepted that ionotropic P2X receptors are expressed in smooth muscle and contribute to vasoconstriction (Matsuura et al., 2004); however recent evidence shows a novel role for P2X activation in endothelium-dependent vasodilation (Harrington et al., 2007). Although there are no known reports, it is possible that CH leads to a decrease in purinergic receptor expression in the pulmonary endothelium. We are unable to completely rule out the possibility that P2X activation leads to membrane depolarization and subsequent Ca^{2+} influx or whether purinergic receptor expression is downregulated following CH. PLC inhibition did, however, abolish residual Ca^{2+} response to ATP in both groups, indicating that P2X receptor activation does not play a role in this response. PKC_{ε} inhibition diminished Ca^{2+} influx similar to T-type channel blockade, suggesting that PKC_{ε} and T-type VGCCs are serially activated, assuming maximal PKC_{ε} inhibition was achieved. Endothelial cells from CH arteries were also insensitive to either of these antagonists and the Ca^{2+} response was strikingly similar to that in control endothelial cells when PKC_{ε} and T-type VGCCs were inhibited, indicating that residual DAG-dependent Ca^{2+} influx pathways may not differ between groups.

Although effects of CH on Ca^{2+} entry have been examined in pulmonary VSM (Jernigan et al., 2007), little is known regarding effects of this stimulus on the endothelium. It is possible that CH decreases endothelial expression of TRP channels to

mediate decreased SOC and ROC entry, but our findings suggest that differential PKC regulation of these pathways more likely contributes to the impaired endothelial Ca^{2+} influx observed in pulmonary hypertension. In conclusion, the present study establishes that there is a generalized decrease in endothelial Ca^{2+} entry in the pulmonary hypertensive vasculature involving PKC that could significantly impair production of endothelium-derived vasodilators. In addition, we provide evidence of a novel PKC-dependent regulation of agonist-induced Ca^{2+} entry that may involve a mibefradil-sensitive Ca^{2+} entry pathway and which is impaired following CH (Figure 8).

Acknowledgements

We would like to thank Minerva Murphy for maintaining the hypobaric chambers utilized in this study.

Reference List

Ahmmed GU, Mehta D, Vogel S, Holinstat M, Paria BC, Tiruppathi C, and Malik AB (2004) Protein kinase Calpha phosphorylates the TRPC1 channel and regulates store-operated Ca2+ entry in endothelial cells. *J Biol.Chem.* **279**:20941-20949.

Albert AP and Large WA (2002) Activation of store-operated channels by noradrenaline via protein kinase C in rabbit portal vein myocytes. *J.Physiol* **544**:113-125.

Arakawa TK, Mlynarczyk M, Kaushal KM, Zhang L, and Ducsay CA (2004) Long-term hypoxia alters calcium regulation in near-term ovine myometrium. *Biol.Reprod.* **71**:156-162.

Chemin J, Mezghrani A, Bidaud I, Dupasquier S, Marger F, Barrere C, Nargeot J, and Lory P (2007) Temperature-dependent modulation of CaV3 T-type calcium channels by protein kinases C and A in mammalian cells. *J.Biol.Chem.* **282**:32710-32718.

Cheng HW, James AF, Foster RR, Hancox JC, and Bates DO (2006) VEGF activates receptor-operated cation channels in human microvascular endothelial cells. *Arterioscler.Thromb.Vasc.Biol.* **26**:1768-1776.

De P, I, Brouns I, Pintelon I, Timmermans JP, and Adriaensen D (2007) Pulmonary expression of voltage-gated calcium channels: special reference to sensory airway receptors. *Histochem.Cell Biol.* **128**:301-316.

Earley S, Straub SV, and Brayden JE (2007) Protein kinase C regulates vascular myogenic tone through activation of TRPM4. *Am.J.Physiol Heart Circ.Physiol* **292**:H2613-H2622.

Ewald DA, Matthies HJ, Perney TM, Walker MW, and Miller RJ (1988) The effect of down regulation of protein kinase C on the inhibitory modulation of dorsal root ganglion neuron Ca2+ currents by neuropeptide Y. *J.Neurosci.* **8**:2447-2451.

Gallegos LL and Newton AC (2008) Spatiotemporal dynamics of lipid signaling: protein kinase C as a paradigm. *IUBMB.Life* **60**:782-789.

Gamberucci A, Giurisato E, Pizzo P, Tassi M, Giunti R, McIntosh DP, and Benedetti A (2002) Diacylglycerol activates the influx of extracellular cations in T-lymphocytes independently of intracellular calcium-store depletion and possibly involving endogenous TRP6 gene products. *Biochem.J* **364**:245-254.

Hardie RC, Peretz A, Suss-Toby E, Rom-Glas A, Bishop SA, Selinger Z, and Minke B (1993) Protein kinase C is required for light adaptation in Drosophila photoreceptors. *Nature* **363**:634-637.

Harrington LS, Evans RJ, Wray J, Norling L, Swales KE, Vial C, Ali F, Carrier MJ, and Mitchell JA (2007) Purinergic 2X1 Receptors Mediate Endothelial Dependent Vasodilation to ATP. *Mol Pharmacol* **72**:1132-1136.

Horibe M, Kondo I, Damron DS, and Murray PA (2001) Propofol attenuates capacitative calcium entry in pulmonary artery smooth muscle cells. *Anesthesiology* **95**:681-688.

Jernigan NL, Broughton BR, Walker BR, and Resta TC (2006) Impaired NO-dependent inhibition of store- and receptor-operated calcium entry in pulmonary vascular smooth muscle after chronic hypoxia. *Am.J.Physiol Lung Cell Mol.Physiol* **290**:L517-L525.

Kim Y, Park MK, Uhm DY, and Chung S (2007) Modulation of T-type Ca2+ channels by corticotropin-releasing factor through protein kinase C pathway in MN9D dopaminergic cells. *Biochem.Biophys.Res.Commun.* **358**:796-801.

Lee H, Suh BC, and Kim KT (1997) Feedback regulation of ATP-induced Ca2+ signaling in HL-60 cells is mediated by protein kinase A- and C-mediated changes in capacitative Ca2+ entry. *J Biol.Chem.* **272**:21831-21838.

Leung PC, Cheng KT, Liu C, Cheung WT, Kwan HY, Lau KL, Huang Y, and Yao X (2006) Mechanism of non-capacitative Ca2+ influx in response to bradykinin in vascular endothelial cells. *J Vasc.Res.* **43**:367-376.

Ma R, Kudlacek PE, and Sansom SC (2002) Protein kinase Calpha participates in activation of store-operated Ca2+ channels in human glomerular mesangial cells. *Am J Physiol Cell Physiol* **283**:C1390-C1398.

Matsuura M, Saino T, and Satoh Yi (2004) Response to ATP is accompanied by a Ca2+ influx via P2X purinoceptors in the coronary arterioles of golden hamsters. *Archives of Histology and Cytology* **67**:95-105.

Montero M, Garcia-Sancho J, and Alvarez J (1993) Inhibition of the calcium store-operated calcium entry pathway by chemotactic peptide and by phorbol ester develops

gradually and independently along differentiation of HL60 cells. *J Biol.Chem.* **268**:26911-26919.

Paffett ML, Naik JS, Resta TC, and Walker BR (2007) Reduced store-operated Ca2+ entry in pulmonary endothelial cells from chronically hypoxic rats. *Am J Physiol Lung Cell Mol.Physiol* **293**:L1135-L1142.

Park JY, Jeong SW, Perez-Reyes E, and Lee JH (2003) Modulation of Ca(v)3.2 T-type Ca2+ channels by protein kinase C. *FEBS Lett.* **547**:37-42.

Park JY, Kang HW, Moon HJ, Huh SU, Jeong SW, Soldatov NM, and Lee JH (2006) Activation of protein kinase C augments T-type Ca2+ channel activity without changing channel surface density. *J Physiol* **577**:513-523.

Pedersen SF and Nilius B (2007) Transient receptor potential channels in mechanosensing and cell volume regulation. *Methods Enzymol.* **428**:183-207.

Pocock TM, Foster RR, and Bates DO (2004) Evidence of a role for TRPC channels in VEGF-mediated increased vascular permeability in vivo. *Am J Physiol Heart Circ Physiol* **286**:H1015-H1026.

Rigual R, Cachero MT, Rocher A, and Gonzalez C (1999) Hypoxia inhibits the synthesis of phosphoinositides in the rabbit carotid body. *Pflugers Arch.* **437**:839-845.

Schuhmann K and Groschner K (1994) Protein kinase-C mediates dual modulation of L-type Ca2+ channels in human vascular smooth muscle. *FEBS Lett.* **341**:208-212.

Trebak M, St JB, McKay RR, Birnbaumer L, and Putney JW, Jr. (2003) Signaling mechanism for receptor-activated canonical transient receptor potential 3 (TRPC3) channels. *J.Biol.Chem.* **278**:16244-16252.

Uenoyama M, Ogata S, Nakanishi K, Kanazawa F, Hiroi S, Tominaga S, Seo A, Matsui T, Kawai T, and Suzuki S (2010) Protein kinase C mRNA and protein expressions in hypobaric hypoxia-induced cardiac hypertrophy in rats. *Acta Physiol (Oxf)* **198**:431-440.

Venkatachalam K, Zheng F, and Gill DL (2003) Regulation of canonical transient receptor potential (TRPC) channel function by diacylglycerol and protein kinase C. *J.Biol.Chem.* **278**:29031-29040.

Wei Z, Manevich Y, Al Mehdi AB, Chatterjee S, and Fisher AB (2004) Ca2+ flux through voltage-gated channels with flow cessation in pulmonary microvascular endothelial cells. *Microcirculation.* **11**:517-526.

Wu S, Haynes J, Jr., Taylor JT, Obiako BO, Stubbs JR, Li M, and Stevens T (2003) Cav3.1 (alpha1G) T-type Ca2+ channels mediate vaso-occlusion of sickled erythrocytes in lung microcirculation. *Circ.Res.* **93**:346-353.

Yang J and Tsien RW (1993) Enhancement of N- and L-type calcium channel currents by protein kinase C in frog sympathetic neurons. *Neuron* **10**:127-136.

Yang M, Ding X, and Murray PA (2008) Differential effects of intravenous anesthetics on capacitative calcium entry in human pulmonary artery smooth muscle cells. *Am J Physiol Lung Cell Mol.Physiol* **294**:L1007-L1012.

Zhang F, Wen Q, Mergler S, Yang H, Wang Z, Bildin VN, and Reinach PS (2006) PKC isoform-specific enhancement of capacitative calcium entry in human corneal epithelial cells. *Invest Ophthalmol.Vis.Sci.* **47**:3989-4000.

Zhou C, Chen H, Lu F, Sellak H, Daigle JA, Alexeyev MF, Xi Y, Ju J, van Mourik JA, and Wu S (2007) Cav3.1 ({alpha}1G) controls von Willebrand factor secretion in rat pulmonary microvascular endothelial cells. *Am J Physiol Lung Cell Mol Physiol* **292**:L833-L844.

Footnotes

This work is supported by American Heart Association [0615551Z] and National Institutes of Health [HL-58124, HL-63207, HL-77876, HL88192].

JPET Fast Forward. Published on June 24, 2010 as DOI: 10.1124/jpet.110.165563
This article has not been copyedited and formatted. The final version may differ from this version.

Legends for Figures

Figure 1. Experimental protocol depicting assessment of endothelial SOC and ROC entry. SOC entry was defined by a change in F_{340}/F_{380} (ΔR) in freshly isolated endothelial cells depleted of intracellular Ca^{2+} stores with 10 μM CPA prior to the re-addition of extracellular Ca^{2+}. Endothelial ROC entry was defined similarly and assessed by application of OAG (100 μM) or ATP (20 μM) following the stabilization of the SOC response. Depolarization-induced entry was assessed in a likewise fashion with high extracellular K^+. PKC, PLC and Ca^{2+} channel inhibitors were administered in separate protocols

Figure 2. PKC inhibition restores endothelial SOC and OAG-induced ROC entry in endothelial cells from CH rats. Endothelial SOC entry was measured as a change in 340/380 (ΔR) fluorescence upon repletion of extracellular Ca^{2+} (1.8 mM) in the presence or absence of the non-selective PKC inhibitor GF109203X **(A)**. Serial assessment of endothelial ROC entry was performed by evaluating OAG-induced Ca^{2+} entry (ΔR) following the SOC response in the presence or absence of GF109203X **(B)**. Values are mean ± SE; *n* is number of endothelial sheets (40-100 cells/sheet) and indicated within data bars; * $P \leq 0.05$ vs. control vehicle; ** vs. CH vehicle.

Figure 3. PKC inhibition blunts ATP-induced Ca^{2+} influx in endothelium from controls, but not from CH pulmonary arteries. ATP-induced Ca^{2+} entry (ΔR) was assessed following the SOC response in the presence of vehicle; the non-selective PKC inhibitor, GF-109203X (1 μM); the PKC_{ε} inhibitor, V1-2myr (10 μM); or the $PKC_{\alpha/\beta}$ inhibitor, Gö6976 (6 nM). Values are mean ± SE; *n* is number of endothelial sheets (40-100

cells/sheet) and indicated within data bars; $P \leq 0.05$ * vs. control vehicle; ** vs. control vehicle.

Figure 4. Receptor-mediated (ATP) Ca^{2+} influx involves T-type VGCCs in endothelium from controls, but not CH pulmonary arteries. Experiments were conducted following the SOC response in the presence of VGCC inhibitors: 10 μM mibefradil, 50 μM diltiazem, or 20 μM SKF96365 **(A)**. Values are mean ± SE; *n* = 5/group; * $P \leq 0.05$ vs respective control; ** vs control vehicle.

Figure 5. Receptor-mediated (ATP) Ca^{2+} influx operates through a PLC-dependent mechanism that potentially requires PKC_ε to activate T-type VGCCs in endothelium from controls, but not CH pulmonary arteries. PLC-dependent signaling through PKC_ε, and T-type VGCCs in ATP-induced Ca^{2+} entry was examined in endothelium from control and CH pulmonary arteries. Experiments were conducted following the SOC entry response in the presence of U73122 (3 μM), U73343 (3 μM), mibefradil (10 μM) and V1-2myr (10 μM). Values expressed as means ± SE; *n* = 5/group; * $P \leq 0.05$ vs inactive analog control; ** vs inactive analog CH; # vs U73343 control.

Figure 6. Endothelial cell Ca^{2+} increases in response to increasing K^+ concentrations. Representative trace illustrating endothelial cell Ca^{2+} response to incremental K^+ concentrations measured by fura-2 in control cells **(A)**. Summary data illustrating K^+-dependent Ca^{2+} responses in endothelium from control and CH pulmonary arteries. KCl-induced Ca^{2+} responses were less at all K^+ concentrations in cells from CH rats compared to controls **(B)**. K^+-induced Ca^{2+} influx was also performed in the presence of the K^+-selective ionophore valinomycin (5 μM) **(C)**. Values expressed as means ± SE; *n* = 4/group; *$P \leq 0.05$ vs. control; **$P \leq 0.05$ vs 15 mM K^+ concentration. Summary data

JPET Fast Forward. Published on June 24, 2010 as DOI: 10.1124/jpet.110.165563
This article has not been copyedited and formatted. The final version may differ from this version.

illustrating reduced Ca^{2+} entry following CH in response to 60 mM K^+ and the effects of VGCC channel inhibition in control endothelial cells. 50 μM diltiazem and 10 μM mibefradil were utilized to selectively inhibit L-type and T-type VGCCs, respectively **(D)**. ΔR defined by change in F340/F380. Values expressed as means ± SE; *n* = 4/group; **P* ≤ 0.05 vs. respective control; ***P* ≤ 0.05 vs. control vehicle and control diltiazem.

Figure 7. Immunofluorescence of $Ca_v3.1$ (α1G) T-type VGCC subunit *(green)* in freshly isolated endothelial cells from small pulmonary arteries harvested from control *(upper row)* and CH *(middle row)* rats (magnification 630x). Images for control *(top)* and CH *(middle)* show detectable $Ca_v3.1$ channel subunit fluorescence (indicated by yellow arrows). Co-incubation with the blocking peptide prevented $Ca_v3.1$ immunofluorescence *(lower left)*. Positive PECAM-1 immunofluorescence shown in blue *(right)* with $Ca_v3.1$ and Sytox nuclear stain in white *(all panels)*.

Figure 8. Diagram depicting the hypothesized effects of CH on purinergic stimulation of a mibefradil-sensitive Ca^{2+} entry pathway via PKC_ε or high extracellular K^+ in pulmonary endothelium from intrapulmonary arteries. Mibefradil (T-type channel blocker), U73122 (PLC inhibitor) and V1-2myr (PKC_ε inhibitor).

JPET Fast Forward. Published on June 24, 2010 as DOI: 10.1124/jpet.110.165563
This article has not been copyedited and formatted. The final version may differ from this version.

Figure 1

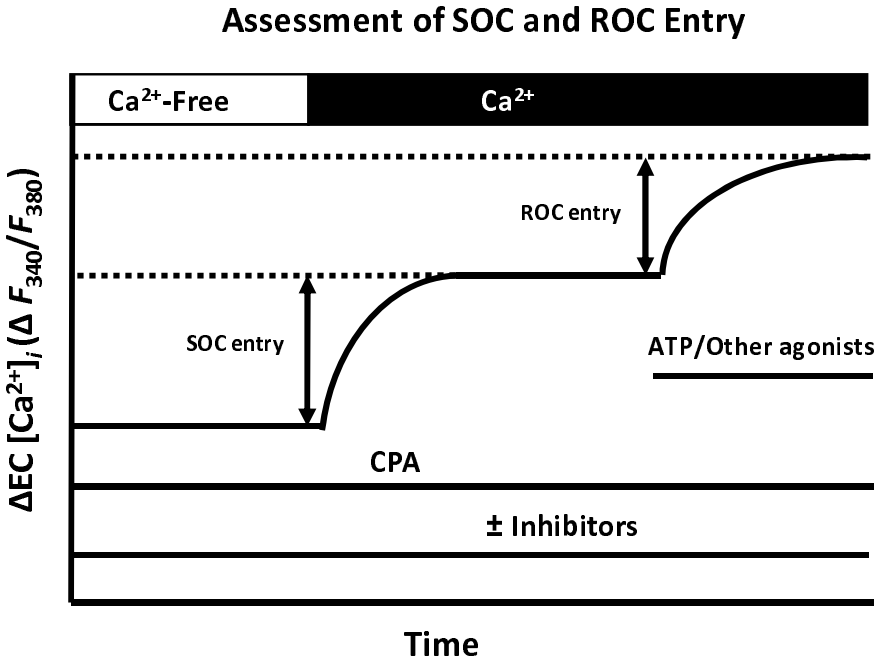

JPET Fast Forward. Published on June 24, 2010 as DOI: 10.1124/jpet.110.165563
This article has not been copyedited and formatted. The final version may differ from this version.

Figure 2

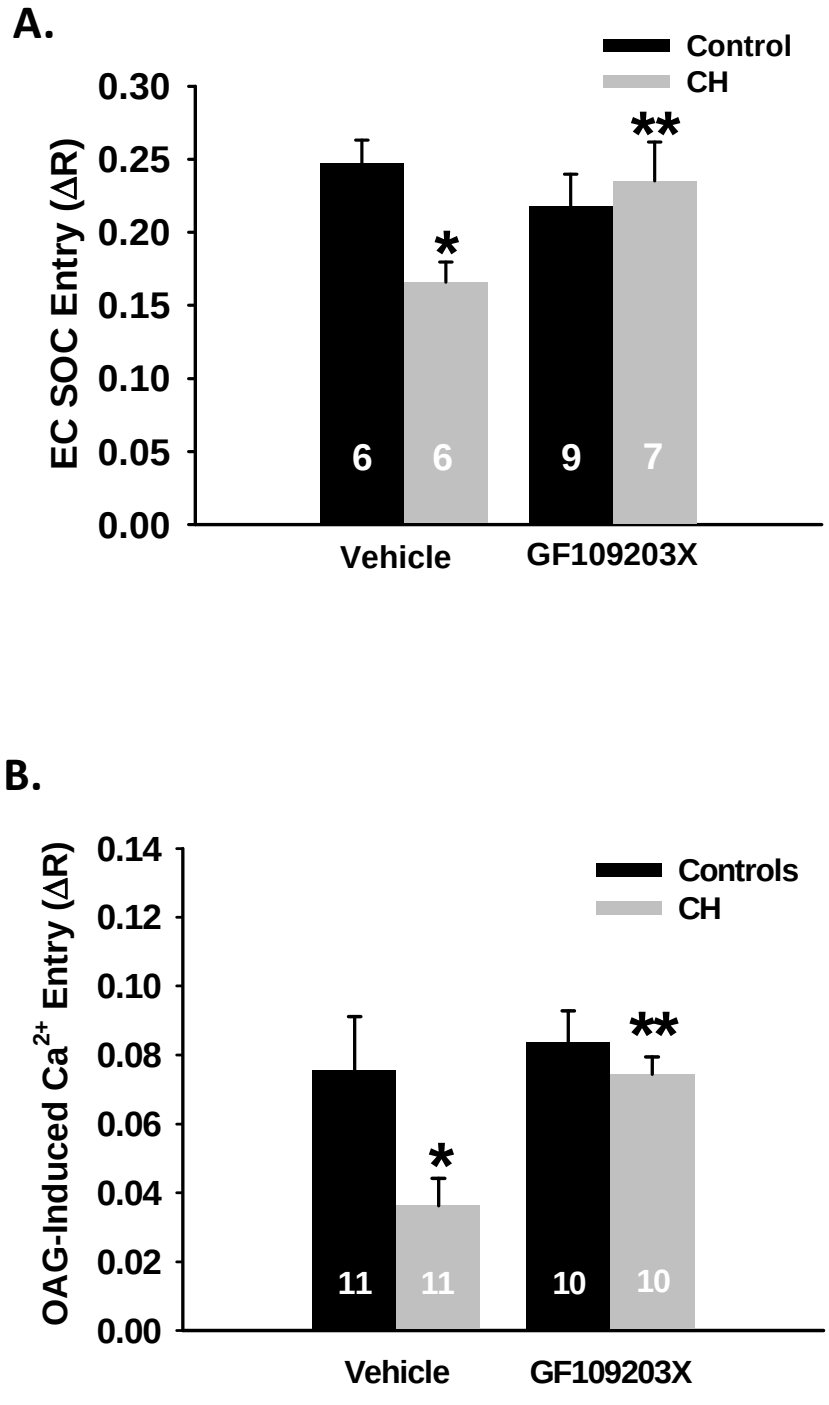

JPET Fast Forward. Published on June 24, 2010 as DOI: 10.1124/jpet.110.165563
This article has not been copyedited and formatted. The final version may differ from this version.

Figure 3

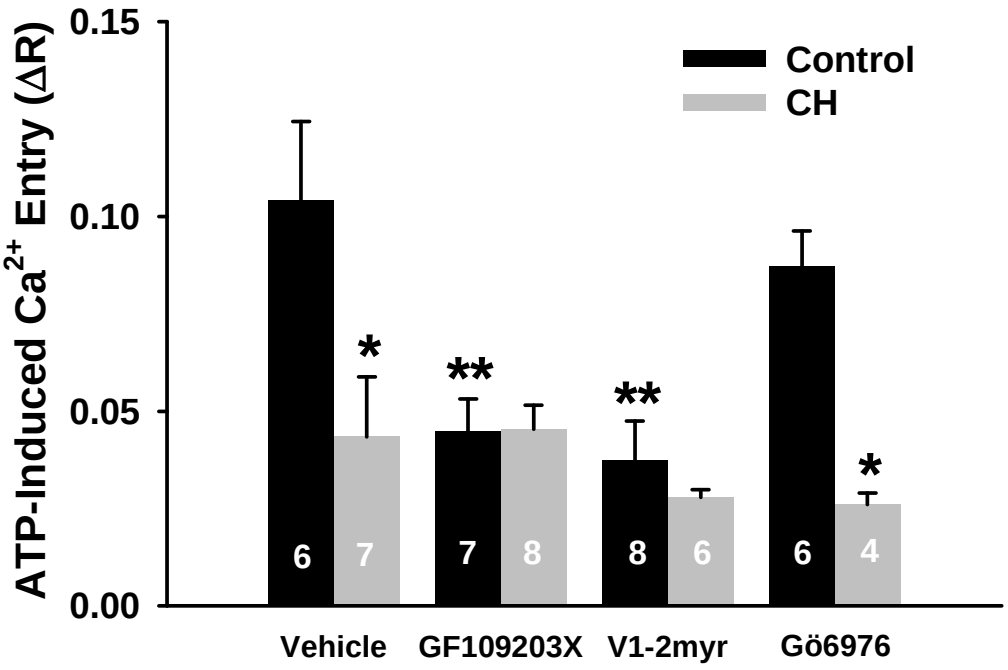

JPET Fast Forward. Published on June 24, 2010 as DOI: 10.1124/jpet.110.165563
This article has not been copyedited and formatted. The final version may differ from this version.

Figure 4

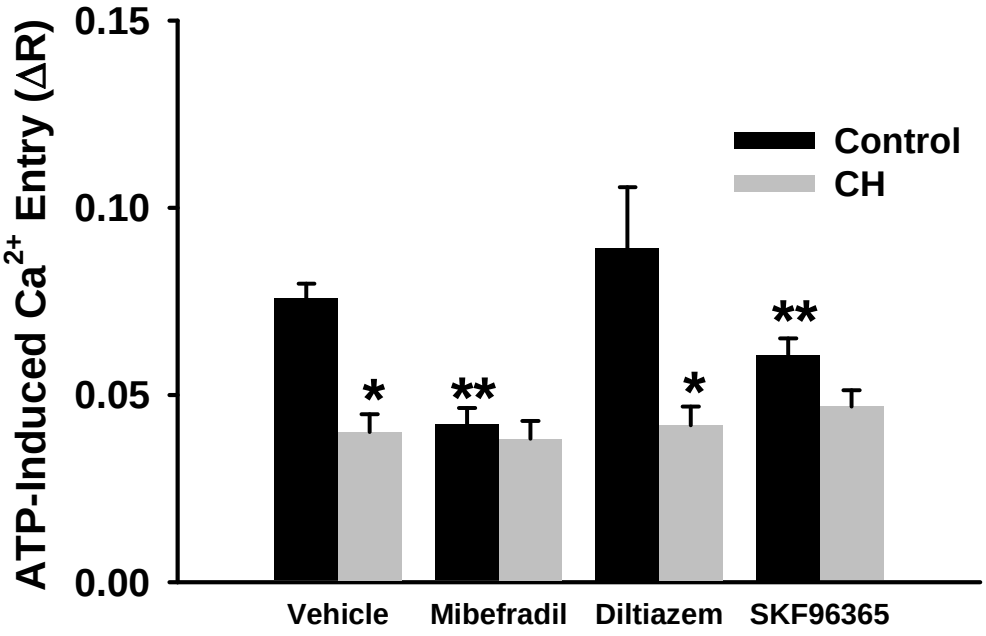

JPET Fast Forward. Published on June 24, 2010 as DOI: 10.1124/jpet.110.165563
This article has not been copyedited and formatted. The final version may differ from this version.

Figure 5

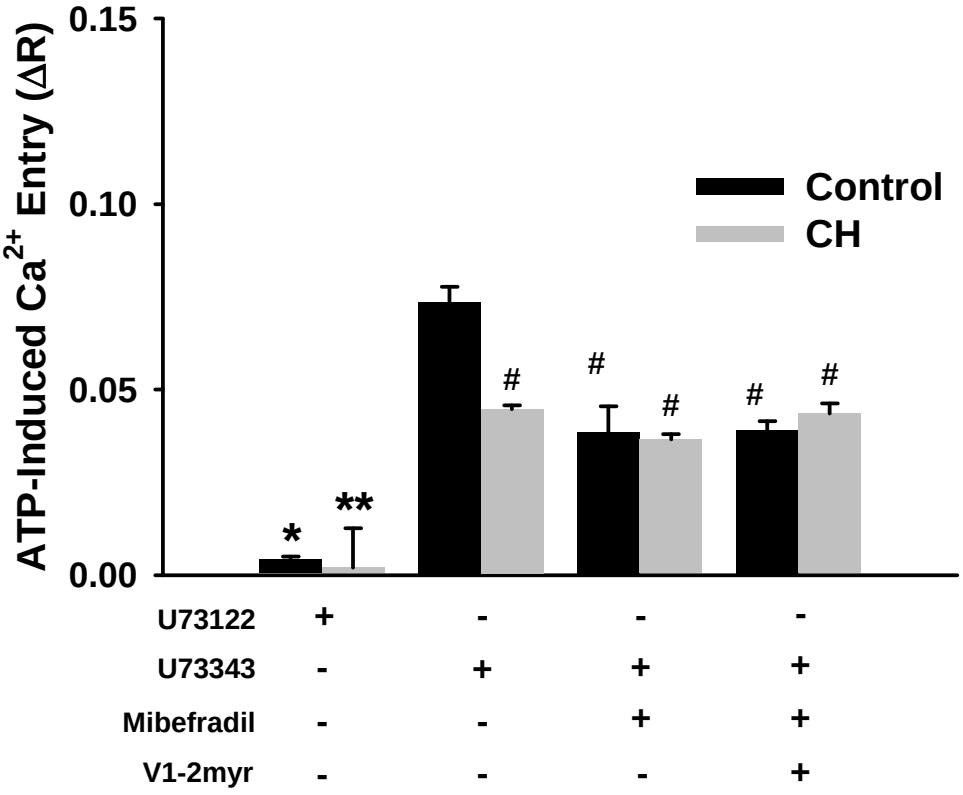

JPET Fast Forward. Published on June 24, 2010 as DOI: 10.1124/jpet.110.165563
This article has not been copyedited and formatted. The final version may differ from this version.

Figure 6

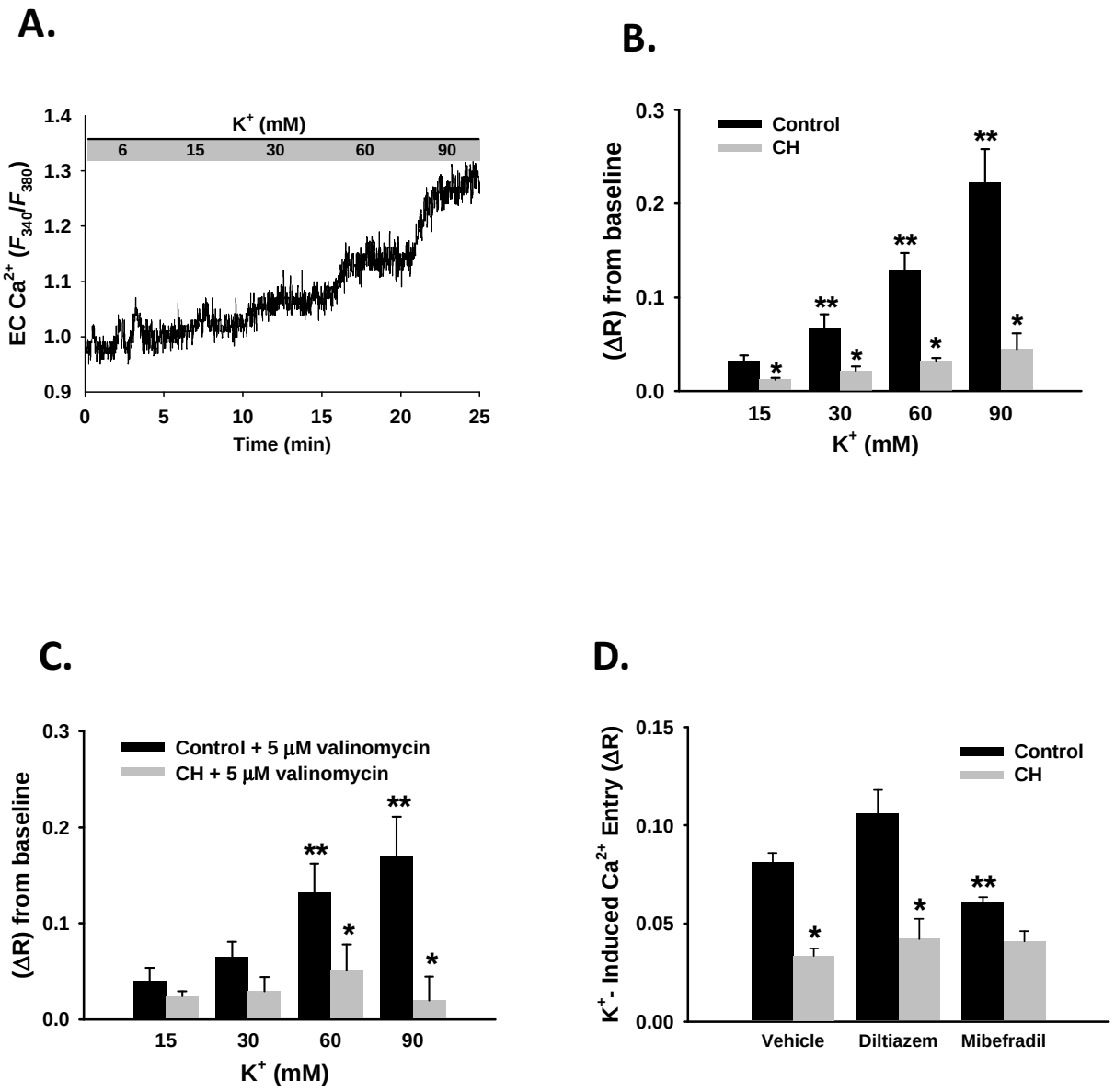

JPET Fast Forward. Published on June 24, 2010 as DOI: 10.1124/jpet.110.165563
This article has not been copyedited and formatted. The final version may differ from this version.

Figure 7

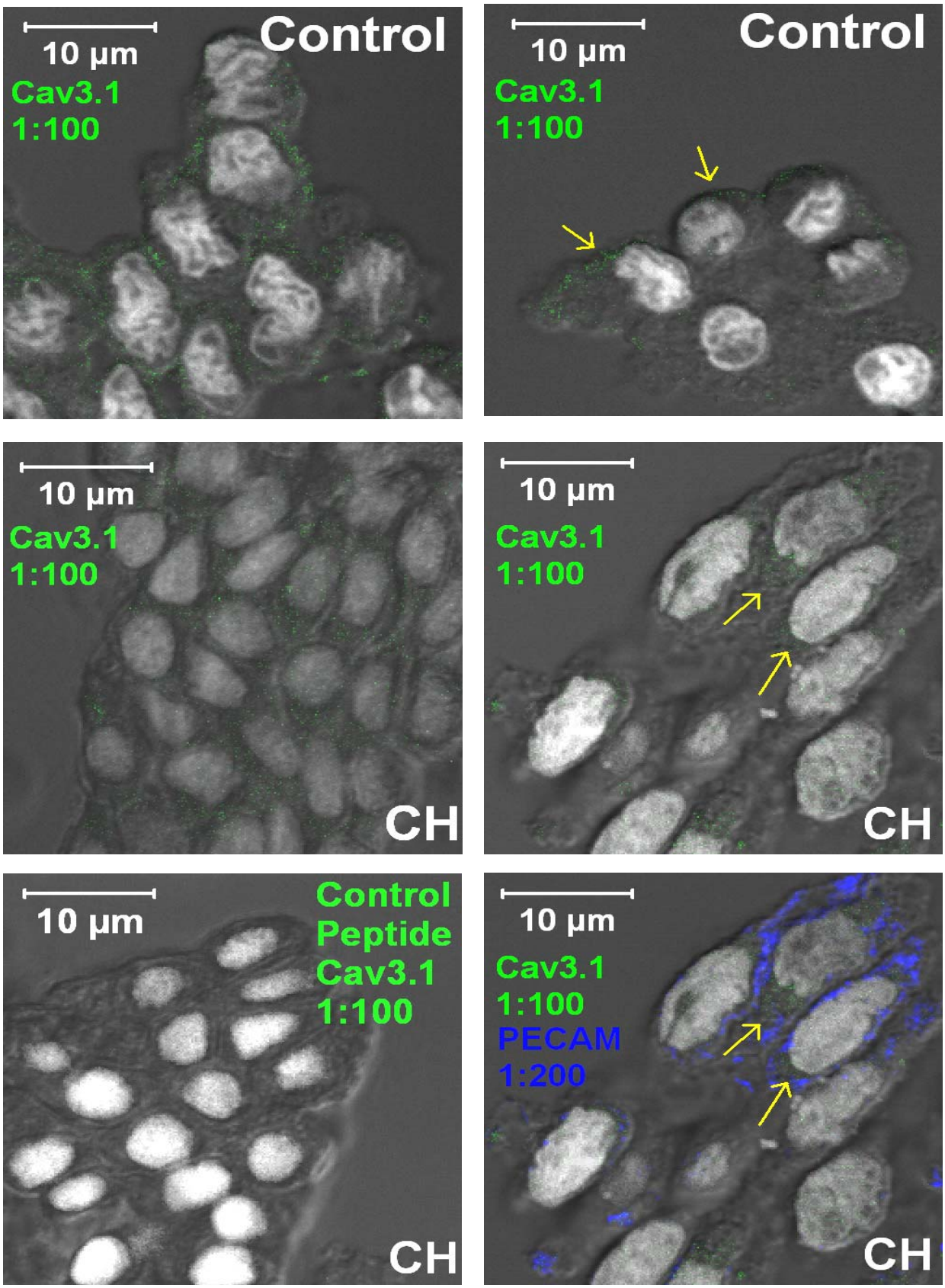

Figure 8

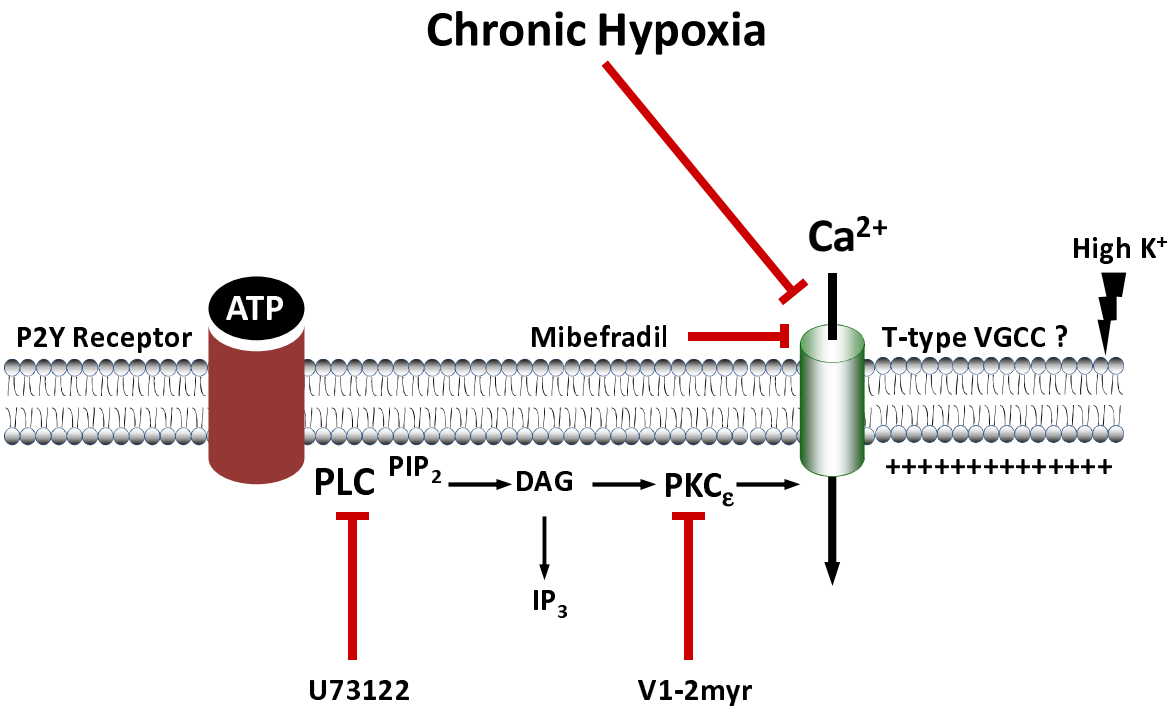

Altered PKC Regulation of Pulmonary Endothelial Store- and Receptor-Operated Ca^{2+} Entry Following Chronic Hypoxia

Michael L. Paffett, Melissa A. Riddle, Nancy L. Kanagy, Thomas C. Resta and Benjimen R. Walker

Journal of Pharmacology and Experimental Therapeutics

Supplemental Figure 1

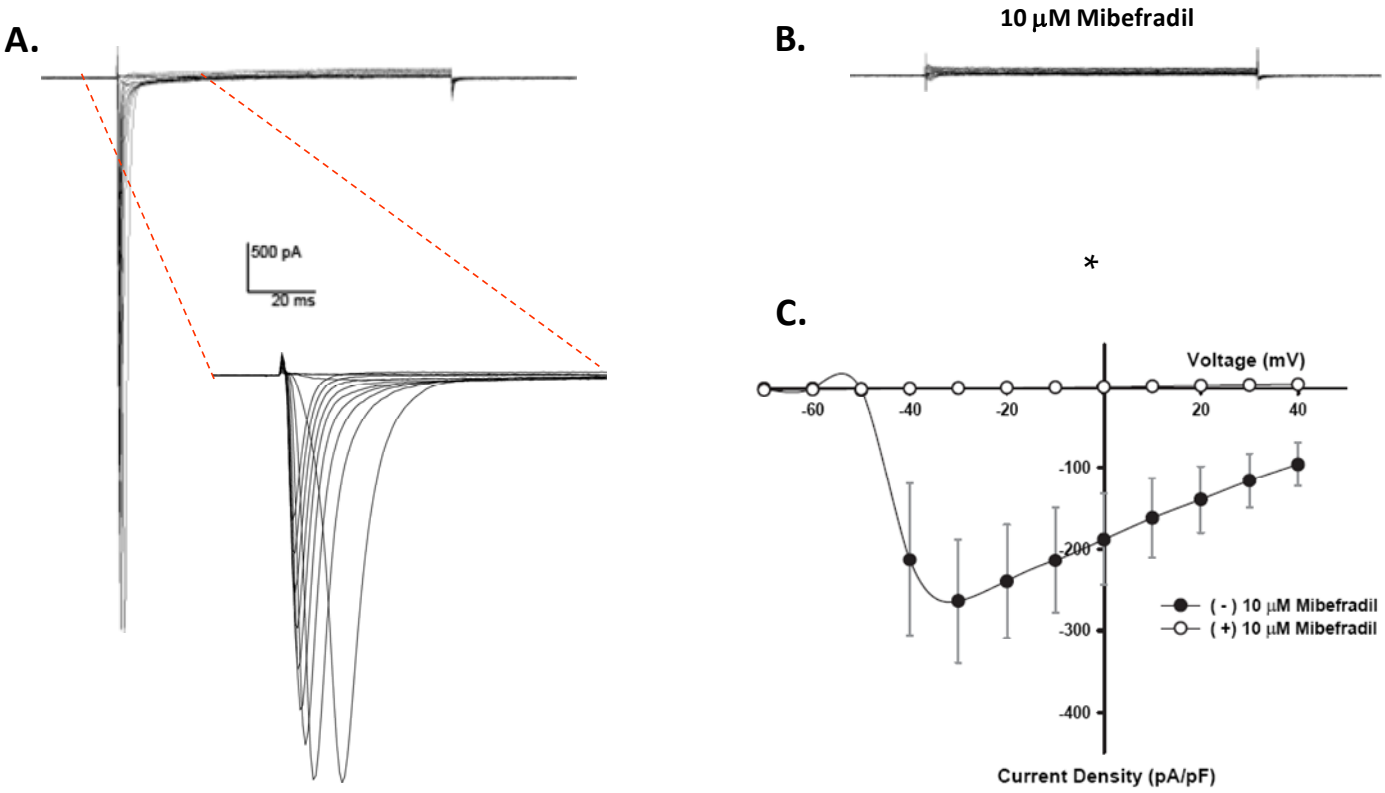

Supplemental Figure 2

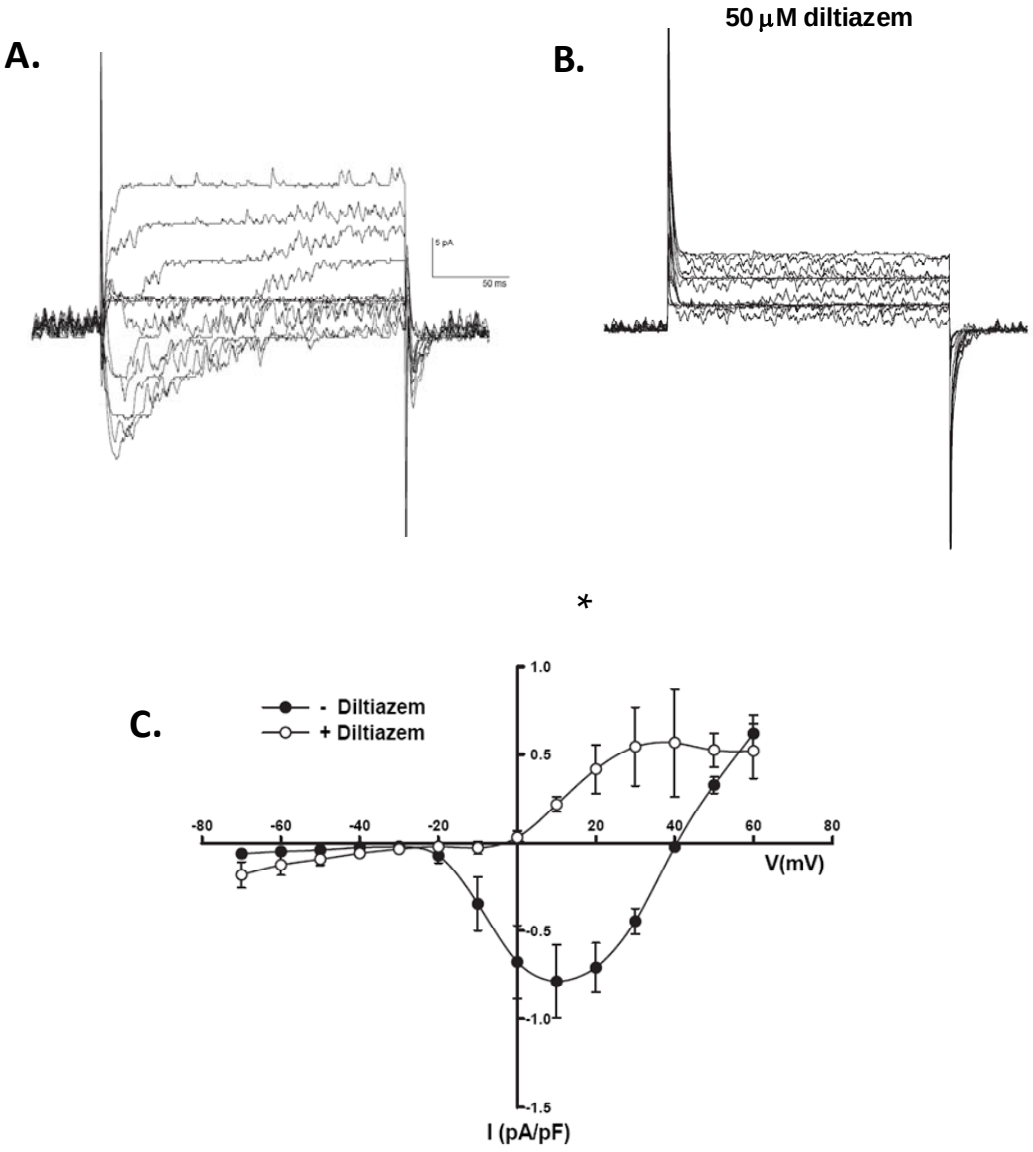

Supplemental Figure Legends

Supplemental Figure 1. T-type voltage-gated Ca^{2+} channel (VGCC) inhibition with mibefradil in neonatal rat ventricular myocytes (NRVM). The whole cell-attached patch clamp method was used to examine the relative characteristics of native NRVM T-type VGCCs. A) Voltage-dependent Ca^{2+} currents ($I_{Ca^{2+}}$) were evoked in NRVM by a voltage pulse protocol and demonstrated relatively rapid activation-inactivation profiles *(see inset)*. Scale bars set for inset blow-up panel. B) Mibefradil (10 μM) completely abolished $I_{Ca^{2+}}$ in NRVMs. C) Current-voltage relationship illustrating a low threshold voltage-dependent activation of mibefradil-sensitive $I_{Ca^{2+}}$. Summary expressed as mean ± SEM (n = 4). $^{*}P \leq 0.05$ from -40 to +40 mV repeated-measures ANOVA.

Supplemental Figure 2. Inhibition of L-type VGCCs with diltiazem in freshly isolated pulmonary artery smooth muscle cells. Whole-cell ($I_{Ca^{2+}}$) evoked from depolarizing voltage steps depict a voltage-dependent inward current (A) which is inhibited with 50 μM diltiazem (B). Summary data (C) illustrate a peak inward current at +10 mV *(closed circles)* and inhibition with diltiazem *(open circles)*, both indicative of L-type VGCCs. Summary expressed as mean ± SEM (n = 4). $^{*}P \leq 0.05$ from -10 to +40 mV repeated-measures ANOVA.

Article Title: Altered PKC Regulation of Pulmonary Endothelial Store- and Receptor-Operated Ca^{2+} Entry Following Chronic Hypoxia

Michael L. Paffett, Melissa A. Riddle, Nancy L. Kanagy, Thomas C. Resta and Benjimen R. Walker

Supplemental Methods

Ventricular Myocyte and Smooth Muscle Cell Isolation

Six day old rat pups (Sprague-Dawley) were euthanized by decapitation and the ventricular myocardium rapidly removed and placed in ice-cold Ca^{2+} and Mg^{2+}-free rodent Ringer solution containing (in mM): 155 NaCl. 5 KCl, 11 glucose, 20 taurine, 10 HEPES adjusted with NaOH to pH 7.4. Ventricles were minced and enzymatically digested at 37°C for 1 hr with the addition of collagenase type IA (1 mg/ml). Freshly dispersed myocytes were centrifuged (300 x g) and the remaining pellet was re-suspended in a 2:1 mixture of Dulbecco's modified Eagle-HAMS F-12 medium containing 10% FBS. Neonatal rat ventricular myocytes (NRVM) were subsequently passed through a 70 μm cell strainer (BD Biosciences) and allowed to seed for 24 hrs prior to measuring Ca^{2+} currents.

The left lungs from adult male Sprague-Dawley rats were rapidly excised following a lethal injection of sodium pentobarbital (200 mg kg^{-1} i.p.) and placed in HEPES buffered saline solution (HBSS). Intrapulmonary arteries were rapidly dissected cut into 2 mm segments and placed in an ice-cold Ca^{2+}-free solution of the following composition (in mM): 60 NaCl, 85 sodium glutamate, 5.6 KCl, $MgCl_2$, glucose, HEPES, NaOH to pH 7.4. After a 10 min equilibration (37°C), artery segments were placed in Ca^{2+}-free isolation solution (37°C) containing 1 mg/ml albumin, 0.7 mg/ml papain and 1 mg/ml DTT. After 40 min exposure to papain, artery segments were placed for 10–15 min in a second isolation solution containing 0.1 mM $CaCl_2$ and a type II collagenase and hyaluronidase mixture (1 mg/ml each). The tissue was subsequently washed twice (10 min each) in Ca^{2+}-free isolation solution and triturated with a polished wide-bore pipet. Pulmonary artery smooth muscle cells (PASMC) were stored on ice and used the same day.

Electrophysiological Recordings of Voltage-Dependent I_{Ca}

Voltage-dependent Ca^{2+} currents were examined in acute (24 hr) primary NRVM cultures or freshly isolated PASMCs using the conventional whole-cell patch clamp technique. Extracellular recording solution contained the following (in mM): 125 NaCl, 6 CsCl, 10 $CaCl_2$, 5 HEPES, 10 TEA-Cl, 5 sucrose, NaOH to pH 7.4. Electrodes with tip resistances of 4-6 MΩ were filled with an intracellular recording solution (in mM): 130 CsCl, 2 Mg-ATP, 1 $MgCl_2$, 5 HEPES, 5 EGTA, CsOH to pH 7.2. After obtaining successful whole-cell configuration, NRVM or PASMC E_m was clamped at a holding potential of –90 mV. Voltage pulses from -70 mV to +60 mV were generated using pClamp software (version 8.6) integrated with an Axopatch200B amplifier (Molecular Devices). Whole-cell capacitance and leak currents were compensated prior to initiating voltage pulse protocols. Because NRVMs are tetrototoxin insensitive (Nuss and Marban, 1994) and abundantly express T-type VGCC (Horiba et al., 2008) we utilized these cells to assess the specificity of the putative inhibitor, mibefradil (10 uM). In addition, freshly isolated PASMCs are known express L-type VGCCs and were utilized to assess the inhibitory action of the recognized L-channel blocker diltiazem. All data were analyzed off-line using Clampfit software (version 9.0)

References Cited

Nuss HB, Marban (1994) Electrophysiological properties of neonatal mouse cardiac myocytes in primary culture. *J. Physiol.* **479**:265-79.

Horiba M, Muto T, Ueda N, Opthof T, Miwa K, Hojo M, Lee JK, Kamiya K, Kodama I, Yasui K **(**2008) T-type Ca2+ channel blockers prevent cardiac cell hypertrophy through an inhibition of calcineurin-NFAT3 activation as well as L-type Ca2+ channel blockers. *Life Sci.* **11-12**:554-60.